Valence band structure of BaCuSF and BaCuSeF

Hiroshi Yanagi[a] and Janet Tate[b]
Department of Physics, Oregon State University, Corvallis, Oregon 97331

Sangmoon Park,[c] Cheol-Hee Park,[d] and Douglas A. Keszler
Department of Chemistry, Oregon State University, Corvallis, Oregon 97331

Masahiro Hirano and Hideo Hosono
Frontier Collaborative Research Center, Tokyo Institute of Technology, 4259 Nagatsuta, Midori-ku, Yokohama 226-8503, Japan and ERATO-SORST, JST, Frontier Collaborative Research Center, Tokyo Institute of Technology, 4259 Nagatsuta, Midori-ku, Yokohama 226-8503, Japan

(Received 7 September 2005; accepted 9 August 2006; published online 23 October 2006)

The origin of high hole conduction in BaCuQF (Q=S,Se) was investigated by photoemission measurements and full-potential linearized augmented plane wave band-structure calculations. In both compounds, the large dispersion near the top of the valence band is realized by admixed states of Cu 3*d* and S 3*p* or Se 4*p* orbitals, indicating that high hole mobility is possible. In addition, the valence band maxima of BaCuQF are much closer to the vacuum level than most *p*-type transparent oxides, which leads to high hole stability in the valence band. The high hole mobility and stability in BaCuQF relative to most oxides afford a significantly larger *p*-type conductivity. © *2006 American Institute of Physics*. [DOI: 10.1063/1.2358828]

I. INTRODUCTION

p-type conductivity in wide band gap semiconductors is a topic relevant to the continued development of transparent electronics and optoelectronics. *n*-type conductivity is readily achieved by appropriate doping in wide band gap oxides such as In_2O_3 and ZnO, where Sn and Al dopings respectively produce conductivities of order 10^3–10^4 S/cm in In_2O_3:Sn and ZnO:Al.[1] Such conductivities in transparent (>80% transmission) films are possible because of the relatively high mobilities of the electrons introduced into the conduction band. These high mobilities [55 $cm^2/V\,s$ in In_2O_3:Sn (Ref. 2) and 120 $cm^2/V\,s$ in ZnO:Al (Ref. 3)] are derived from the strong *s* orbital character in the conduction bands, which leads to wide, dispersed bands and relatively low effective masses. In contrast, *p*-type conductivity in wide band gap materials has been more difficult to achieve. The delafossite compounds CuMO$_2$ (M=Al,Ga,In,Sc,Y) are a family of *p*-type conductors,[4–8] but conductivities of transparent native-doped materials are small (1 S/cm or less) and doping is either difficult or compromises transparency to a greater extent for a given conductivity than is the case for the *n*-type counterparts. Low mobilities in these materials ($\leqslant$0.1 $cm^2/V\,s$) result from extremely narrow valence bands with strong Cu 3*d* character near the top of the valence band.[9] More promising candidates are wide band gap chalcogenide-fluorides, such as BaCuSF and BaCuSeF,[10] and oxide-chalcogenides, such as LaCuOS$_{1-x}$Se$_x$,[11] which have similar structures. Conductivities in these materials have been reported to be as high as 100 S/cm for BaCuQF (Q=S,Se) (Ref. 10) and 140 S/cm for LaCuOSe.[11] The mobilities are several orders of $cm^2/V\,s$ for undoped LaCuOSe,[11] and also for BaCuSF.[12] This indicates that the top of the valence band must have weaker Cu 3*d* character in comparison with the oxides. Given the similarity of the condensation of CuS_4 tetrahedra in BaCuQF to those in the related $BaCu_2S_2$, also a *p*-type conductor with a mobility of about 3 $cm^2/V\,s$,[13] it is highly likely that the S 3*p* and Se 4*p* orbitals contribute to the top of the valence band. Support for this conjecture is presented in this paper on the basis of results from electron photoemission experiments as well as band-structure calculations for theoretical support.

II. EXPERIMENTS

Undoped BaCuQF (Q=S,Se) disks were prepared by conventional solid-state techniques. Full details have been reported elsewhere.[10] Sulfide-fluoride powder samples were prepared by heating stoichiometric mixtures of the reagents $BaCO_3$ (Cerac, 99.9%), Cu_2S (Cerac, 99.5%), and BaF_2 (Cerac, 99.9%) at 550 °C for 1 h under a flowing stream of H_2S (g) and cooling to room temperature under flowing Ar (g). Powder samples of BaCuSeF were prepared by heating stoichiometric mixtures of BaSe (Cerac, 99.5%), Cu_2Se (Cerac, 99.5%), and BaF_2 (Cerac, 99.9%) at 450–550 °C for 12 h in an evacuated silica tube. The powders are stable in ambient conditions, but are water sensitive. All samples were characterized by powder x-ray diffraction and contained only trace impurities. Each powder sample was pressed into a pellet and annealed at 650 °C for 1 h in an evacuated silica tube. The BaCuSF and BaCuSeF pellet densities were 73% and 76% of theoretical density, respectively.

Photoemission spectroscopy measurements were performed at room temperature on the polycrystalline pellet samples. The electrical conductivities of the BaCuSF and BaCuSeF pellets were 0.09 and 0.06 S/cm, respectively, and

[a]Present address: Materials and Structures Laboratory, Tokyo Institute of Technology, 4259 Nagatsuta, Midori-ku, Yokohama 226-8503, Japan.
[b]Electronic mail: tate@physics.oregonstate.edu
[c]Present address: Department of Chemistry and USC Nanocenter, University of South Carolina, SC 29208, Columbia.
[d]Present address: LG Chem Research Park, Daejeon 305-380, South Korea.

p-type conductivity was established for each material through the Seebeck effect with coefficients measured as +56 and +32 μV/K, respectively.[10] Clean sample surfaces were obtained by polishing with a diamond file in the sample preparation chamber under 3×10^{-9} Torr, after which, samples were transferred into the measurement chamber whose base pressure was 5×10^{-10} Torr. The excitation light sources used in this study were He I and He II resonances (21.2 eV for He I and 40.8 eV for He II) and the Mg $K\alpha$ x-ray emission (1254 eV). A sample bias of −5 V was applied during the measurements of He I spectra.[14] A hemispherical analyzer and a single channeltron were used for detection of photoelectrons. Because the work function is sensitive to surface conditions, the He I spectra that determine work functions were measured within 15 min of polishing. All spectra were measured under a vacuum of 10^{-9} Torr.

Energy band calculations for BaCuSF and BaCuSeF were performed by using the full-potential linearized augmented plane wave (FLAPW) method.[15] The space group was $P4/nmm$, and the lattice constants were $a=b=0.4123$ nm and $c=0.9021$ nm for BaCuSF, and $a=b=0.4239$ nm and $c=0.9122$ nm for BaCuSeF. The details of the calculations are as follows. Muffin tin radii of 2.3 a.u. (S) and 2.4 a.u. (Se) were used. The potentials and charge densities in the interstitial region were expanded using 8907 (S) and 9583 (Se) plane waves. Inside the spheres, these quantities were expanded up to $l=8$. The maximum augmented plane wave (APW) wave vector was 4.0 a.u., which resulted in about 1200 basis functions per cell or about 150 basis functions per atom. The APW functions were expanded up to $l=10$. The number of k points used in the calculations was 60. Because the material is an insulator, such a small number was sufficient, which we checked by doing all calculations with 30 k points as well. With these parameters, total energies converged to better than 1 mRy. Numerical errors in the band structure are too small to see in the plots.

III. RESULTS

Major signals in the wide range x-ray photoemission spectroscopy (XPS) spectra (complete spectra not shown here) can all be attributed to the component atoms Ba, Cu, S (or Se), and F, while very small peaks from O 1*s* and C 1*s* orbitals are also evident. The presence of Cu^{2+} in a material can be inferred from the presence of a satellite peak on the high-energy side of the main Cu 2*p* lines at ~933 eV in the XPS spectrum. A typical case is CuO (Ref. 16) with a d^9 configuration in the ground state. The absence of such satellite peaks near 942 eV, however, implies that the concentration of Cu^{2+} in the materials is extremely low.

For the narrow-range valence band spectra shown in Fig. 1, the binding energy is given with respect to the Fermi energy, which was set to zero by using the Fermi edge of Ag. For each material, the Fermi energy lies near the top of the valence band, which agrees with the fact that samples exhibit *p*-type electrical conductivity. In each case, the valence band is characterized by a small feature just below the Fermi level and a more intense peak at a higher binding energy. These

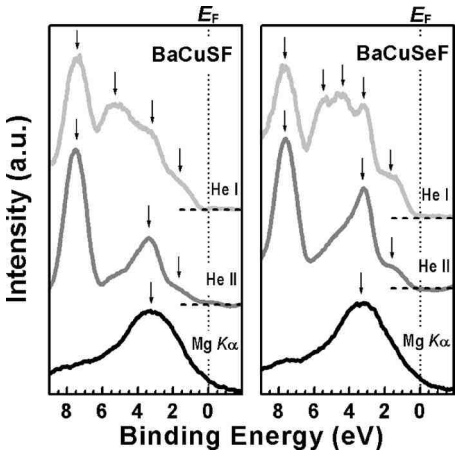

FIG. 1. Photoemission spectra of BaCuSF (left panel) and BaCuSeF (right panel). The excitation energy of each spectrum is 21.2 eV for He I, 40.8 eV for He II, and 1254 eV for XPS. The secondary electron background has been subtracted. The upper valence band is comprised of S 3*p* or Se 4*p*, and Cu 3*d* orbitals.

features are very similar to those in the spectra of transparent *p*-type oxides and oxide chalcogenides.[6,17–19] The following are detailed features in the energy range shown in Fig. 1. As indicated by the arrows, BaCuSF has four peaks present in the He I spectrum, three in the He II spectrum, and one broad peak in the XPS spectrum. In the case of BaCuSeF, there are five peaks in He I spectrum, three peaks in the He II spectrum, and one peak in XPS spectrum. The intensity of each peak changes with the excitation energy of the light source. This allows us to infer something of the nature of the valence band as discussed below. The work functions of BaCuSF and BaCuSeF estimated from He I ultraviolet photoemission spectroscopy (UPS) spectra are 4.3 and 3.6 eV, respectively.

The results of the band-structure calculations are shown in Fig. 2, where the zero is set at the valence band maximum (VBM). A direct gap is indicated from the fact that the conduction band minimum and the valence band maximum are both located at the Γ point. The band structures exhibit relatively large dispersion around the VBM in the Γ to *M* and Γ to *X* directions, and the valence band is rather flat in the Γ to *Z* direction. These results are consistent with the layered nature of the crystal structure, where the Cu–S interactions extend only in the *xy* plane. The total and partial densities of states are plotted to the right of the band structure and also in Fig. 3. The contribution of the Cu 3*d* states to the top of the valence band is strong. As seen from the projected density of states in Fig. 2, the Cu 3*d* levels separate into three distinct regions near 1, 2, and 3.5 eV. In terms of a crystal field model, the top and bottom regions represent the antibonding and bonding components, respectively, of the t_2 set of *d* orbitals, while the middle region corresponds to the more weakly interacting *e* set. The contribution of Cu 3*d* near the top of the valence band is similar to the delafossite structures,[20] but contributions from the S 3*p* or Se 4*p* are also significant. Thus, the observed changes in transport properties, i.e., higher mobilities in the sulfide and selenide relative to the delafossite, are to be expected. Similar properties are found in the band structure and densities of states of LaCuOS.[17–21]

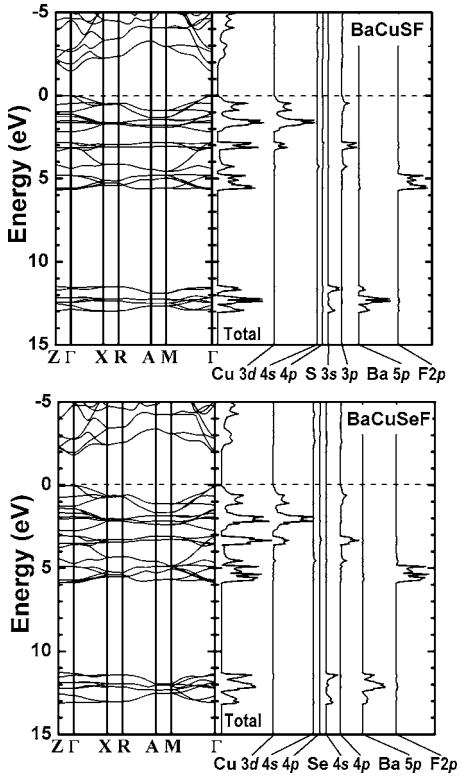

FIG. 2. FLAPW band structure and total and partial density-of-states calculations for BaCuSF (upper panel) and BaCuSeF (lower panel).

The calculation also includes plane wave contributions to the density of states (not plotted). The plane wave contribution to the valence band is relatively small (see Fig. 3), but is important for the conduction band.

IV. DISCUSSION

Signature peaks for Cu 3*d*, S 3*p* (or Se 4*p*), F 2*p*, and Ba 5*p* orbitals are evident in the electron photoemission spectra covering binding energies from 0 to 20 eV. Photoionization cross sections normalized relative to the Cu 3*d* cross section[22] are summarized in Table I. In the XPS spectra, peaks arising from Ba 5*p* and Cu 3*d* orbitals are observed. In the UPS spectra, peaks arising from Cu 3*d*, F 2*p*, and S 3*p* (or Se 4*p*) orbitals for He I, and peaks arising from Cu 3*d*, F 2*p*, and Ba 5*p* orbitals for He II are observed.

TABLE I. Relative photoionization cross sections of Ba 5*p*, Cu 3*d*, S 3*p*, Se 4*p*, and F 2*p* orbitals calculated from theoretical values (Ref. 22 for 21.2 eV (He I), 40.8 eV (He II), and 1.2 keV (Mg). The photoionization cross section of the Cu 3*d* orbital at 40.8 eV was set to 1.

Source (energy)	Ba 5*p*	Cu 3*d*	S 3*p*	Se 4*p*	F 2*p*
He I (21.2 eV)	···	0.7	0.4	0.8	0.9
He II (40.8 eV)	0.2	1	0.06	0.06	0.8
Mg (1253.6 eV)	0.001	0.002	0.0002	0.0004	0.0001

Peak structures near 15 eV (not shown in Fig. 1) in the He II UPS and XPS spectra of BaCu*Q*F (*Q*=S,Se) arise from the Ba 5*p* orbitals. We assign the very strong peaks at ~7.5 eV in the UPS spectra of BaCu*Q*F, which are absent in the XPS spectra, to F 2*p* orbitals. This is based on the fact that the photoionization cross section of the F 2*p* orbitals at 1254 eV is about 10^{-4} times that at 21.2 and 40.8 eV. Whereas the XPS photoionization cross section is small relative to those at UPS energies for all the elements, the strongest suppression occurs for the F 2*p* orbitals, and of the XPS photionization cross sections, the F 2*p* is the smallest.

The relative photoionization cross sections of S 3*p* and Se 4*p* for the excitation energy of 21.2 eV are considerably higher than those of the other excitation energies, cf. Table I. Consequently, peaks arising from these orbitals should be enhanced in the He I spectra. There are three peaks at 1.5, 3.4, and 5.6 eV in the UPS spectra of BaCuSF between 0 and ~6 eV, cf. Fig. 1, and two of these peaks, 1.5 and especially 5.6 eV, are enhanced in the He I spectrum relative to the He II spectrum. Consequently, S 3*p* orbitals contribute to

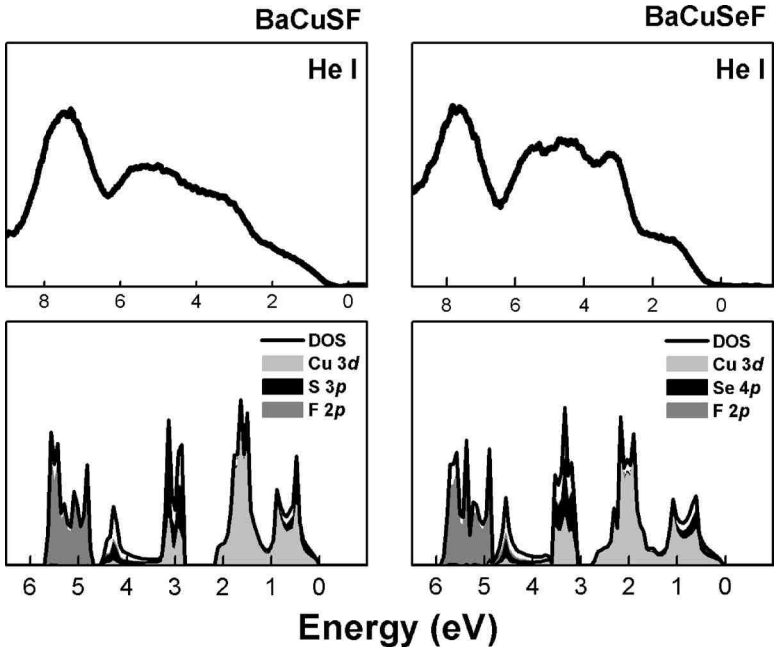

FIG. 3. Comparison of the He I UPS spectrum with the APW band-structure calculations for BaCuSF and BaCuSeF. The calculated partial densities of states are shown for Cu 3*d*, S 3*p* or Se 4*p*, and F 2*p*. The small remainder of the density of states is accounted for by plane wave contributions.

these two peaks. Cu also contributes to each of the three peaks at 1.5, 3.4, and 5.6 eV. Thus, qualitatively, the features of the APW calculation are observed experimentally as shown in Fig. 3. The upper valence band consists of hybrid Cu $3d-S\ 3p$ orbitals of antibonding character, lying slightly above weakly interacting (or nonbonding) orbitals of largely Cu $3d$ character, which in turn are above Cu $3d-S\ 3p$ hybrids of bonding character. Finally, the lowest part of the valence band consists predominantly of F $2p$ states. In the same manner, Se $4p$ and Cu $3d$ orbitals contribute to the peaks between the Fermi energy and ~6 eV in the spectra of BaCuSeF, and again the F $2p$ orbitals form the bottom of the valence band.

Although the photoemission results for BaCuSF bear many similarities to those of LaCuOS, important differences do exist. In LaCuOS, O $2p$ orbitals are a major constituent of half of the valence band, mainly the central section.[18] On the other hand, F $2p$ orbitals in the BaCuQF system contribute only to the lowest part of the valence band (less than one quarter, as seen in Fig. 3). Considered as a quantum well structure, the valence band offset energy of ~6 eV between $(Cu_2Q_2)^{2-}$ and $(Ba_2F_2)^{2+}$ layers in BaCuQF is much larger than the ~1.5 eV between $(Cu_2S_2)^{2-}$ and $(La_2O_2)^{2+}$ in LaCuOS,[18] while the conduction band features are similar. These results are supported by the FLAPW band-structure calculations, where it is seen from the partial-density-of-states projections that the F $2p$ orbitals contribute only to the bottom of the valence band in both BaCuSF and BaCuSeF. Consequently, we expect the anisotropy of transport and optical properties to be much greater in the BaCuQF family than in the LaCuOQ family.

The positions of the Fermi level and valence band maxima relative to the vacuum energy (E_V) are summarized in Fig. 4 along with VBM of typical p-type transparent oxides $CuAlO_2$ and $CuGaO_2$ measured by electrochemical means.[23,24] Conduction band minima were determined with a band gap energy of 3.2 eV for BaCuSF and 3.0 eV for BaCuSeF,[10] and the energy positions of the VBM. The VBM and bandwidths of the valence bands were estimated from UPS spectra. As noted above, the upper part of the valence band is composed of Cu $3d$ orbitals and S $3p$ or Se $4p$ orbitals, and the lower part is composed of F $2p$ orbitals. The VBM of BaCuQF are much shallower (closer to E_V) than those of typical p-type oxides. Since hole carriers are stable in such a shallow position, this diagram explains the experimental observation that BaCuQF (Q=S,Se) shows degenerate conduction by substitutional doping and that a similar doping effect is hardly observed in the wide band gap, p-type transparent oxides $CuAlO_2$ and $CuGaO_2$. As seen in Fig. 4, the energy positions of the conduction band minima are also shallow, indicating that realization of n-type conduction in these compounds will be difficult, despite the contribution of Cu $4s$ orbital character in the bottom of the conduction band.

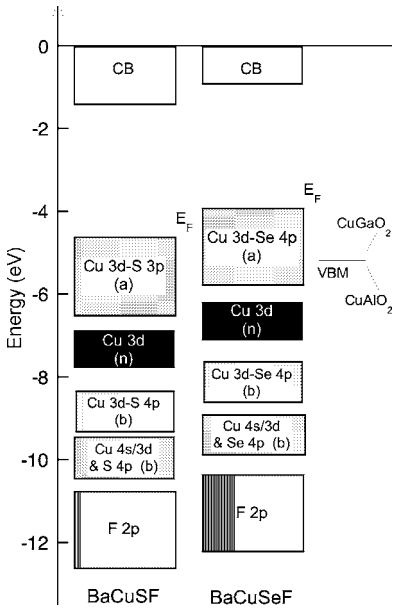

FIG. 4. Schematic band diagrams of BaCuSF and BaCuSeF with VBM of typical p-type transparent oxides, 5.2 eV for $CuAlO_2$ and 5.1 eV for $CuGaO_2$. Work functions and VBM positions from E_V are 4.3 and 4.6 eV for BaCuSF, and 3.6 and 3.9 eV for BaCuSeF, respectively. Conduction band minima were determined with a band gap energy of 3.2 eV for BaCuSF and 3.0 eV for BaCuSeF (Ref. 10), and the energy positions of the VBM. The symbols (b), (n), and (a) denote bonding, nonbonding, and antibonding orbitals, respectively.

V. SUMMARY

Valence band photoemission measurements of BaCuQF and band-structure calculations have revealed the origins of high p-type conductivity in the wide gap, Cu-based chalcogenide fluorides. The upper valence band is primarily composed of a mixture of S $3p$ and Cu $3d$ orbitals for BaCuSF and Se $4p$ and Cu $3d$ orbitals for BaCuSeF. This admixture leads to larger dispersion near the VBM, which translates to a relatively high hole mobility. Furthermore, hole stability is increased by the shallow VBM in BaCuQF, allowing a high hole concentration to be realized. In other words, *both* parameters that control electrical conductivity, carrier concentration, and mobility are improved in BaCuQF relative to wide band gap Cu oxides. The shallow VBM in these compounds is largely associated with the relatively small electron affinities of S and Se and the dispersion that ensues from the mixing of the Cu and S (Se) orbitals. The wide separation of the F orbitals from the top of the valence band indicates that these materials may exhibit exceptional anisotropy in electrical and optical properties, pointing to a need for growth and characterization of single-crystal samples.

ACKNOWLEDGMENTS

We thank Professor Henri J. F. Jansen of Oregon State University for the band-structure calculations. This material is based upon work supported by the National Science Foundation under Grant No. 0245386.

[1]T. Minami, MRS Bull. **25**, 38 (2000).
[2]H. Ohta, M. Orita, M. Hirano, H. Tanji, H. Kawazoe, and H. Hosono, Appl. Phys. Lett. **76**, 2740 (2000).
[3]T. Minami, H. Nanto, and S. Takata, Appl. Phys. Lett. **41**, 958 (1982).
[4]H. Kawazoe, M. Yakusawa, H. Hyodo, M. Kurita, H. Yanagi, and H. Hosono, Nature (London) **389**, 939 (1997).
[5]K. Ueda, T. Hase, H. Yanagi, H. Kawazoe, H. Hosono, H. Ohta, M. Orita, and M. Hirano, J. Appl. Phys. **89**, 1790 (2001).
[6]H. Yanagi, T. Hase, S. Ibuki, K. Ueda, and H. Hosono, Appl. Phys. Lett.

78, 1583 (2001).
[7]N. Duan, M. K. Jayaraj, J. Tate, and A. W. Sleight, Appl. Phys. Lett. **77**, 1325 (2000).
[8]M. K. Jayaraj, A. D. Draeseke, J. Tate, and A. W. Sleight, Thin Solid Films **397**, 244 (2001).
[9]L. F. Mattheiss, Phys. Rev. B **48**, 18300 (1993).
[10]H. Yanagi, J. Tate, S. Park, C.-H. Park, and D. A. Keszler, Appl. Phys. Lett. **82**, 2814 (2003).
[11]H. Hiramatsu, K. Ueda, H. Ohta, M. Hirano, T. Kamiya, and H. Hosono, Appl. Phys. Lett. **82**, 1048 (2003).
[12]R. Kykyneshi, J. Tate, C.-H. Park, and D. A. Keszler (unpublished).
[13]S. Park, D. A. Keszler, M. M. Valencia, R. L. Hoffman, J. P. Bender, and J. F. Wager, Appl. Phys. Lett. **80**, 4393 (2002).
[14]A. Klein, Appl. Phys. Lett. **77**, 2009 (2000).
[15]H. J. F. Jansen and A. J. Freeman, Phys. Rev. B **30**, 561 (1984).
[16]J. Ghijsen, L. H. Tjeng, J. van Elp, H. Eskes, J. Westerink, G. A. Sawatzky, and M. T. Czyzyk, Phys. Rev. B **38**, 11322 (1988).
[17]S. Inoue, K. Ueda, H. Hosono, and N. Hamada, Phys. Rev. B **64**, 245211 (2001).
[18]K. Ueda, H. Hiramatsu, H. Ohta, M. Hirano, T. Kamiya, and H. Hosono, Phys. Rev. B **69**, 155305 (2004).
[19]K. Ueda, H. Hosono, and N. Hamada, J. Phys.: Condens. Matter **16**, 5179 (2004).
[20]H. Yanagi, S. Inoue, K. Ueda, H. Kawazoe, H. Hosono, and N. Hamada, J. Appl. Phys. **88**, 4159 (2000).
[21]K. Ueda, H. Hosono, and N. Hamada, J. Appl. Phys. **98**, 043506 (2005).
[22]J.-J. Yeh, *Atomic Calculation of Photoionization Cross-Sections and Asymmetry Parameters* (Gordon and Breach, Pennsylvania, 1993).
[23]F. A. Benko and F. P. Koffyberg, J. Phys. Chem. Solids **45**, 57 (1984).
[24]F. A. Benko and F. P. Koffyberg, Phys. Status Solidi A **94**, 231 (1986).